Biogeochemistry (2016) 130:247–265
DOI 10.1007/s10533-016-0255-z

Regional meteorological drivers and long term trends of winter-spring nitrate dynamics across watersheds in northeastern North America

Jill Crossman · M. Catherine Eimers · Nora J. Casson · Douglas A. Burns · John L. Campbell · Gene E. Likens · Myron J. Mitchell · Sarah J. Nelson · James B. Shanley · Shaun A. Watmough · Kara L. Webster

Received: 11 March 2016 / Accepted: 27 September 2016 / Published online: 4 October 2016
© Springer International Publishing Switzerland 2016

Abstract This study evaluated the contribution of winter rain-on-snow (ROS) events to annual and seasonal nitrate ($N\text{-}NO_3$) export and identified the regional meteorological drivers of inter-annual variability in ROS $N\text{-}NO_3$ export (ROS-N) at 9 headwater streams located across Ontario, Canada and the northeastern United States. Although on average only 3.3 % of annual precipitation fell as ROS during winter over the study period, these events contributed a significant proportion of annual and winter $N\text{-}NO_3$ export at the majority of sites (average of 12 and 42 %, respectively); with the exception of the most northern catchment, where total winter precipitation was exceptionally low (average 77 mm). In years with a greater magnitude of ROS events, the timing of the peak $N\text{-}NO_3$ export period (during spring melt) was redistributed to earlier in the year. Variability in ROS frequency and magnitude amongst sites was high and a generalised linear model demonstrated that this spatial variability could be explained by interactive effects between regional and site-specific drivers. Snowpack coverage was particularly important for explaining the site-specific ROS response. Specifically, ROS events were less common when higher temperatures eliminated snow cover despite increasing the proportion of winter rainfall, whereas ROS event frequency was greater at sites where sufficient snow cover remained.

Responsible Editor: Jacques C. Finlay

Electronic supplementary material The online version of this article (doi:10.1007/s10533-016-0255-z) contains supplementary material, which is available to authorized users.

J. Crossman (✉) · M. Catherine Eimers
School of the Environment, Trent University, West Bank Drive, Peterborough, ON K9J 7B8, Canada
e-mail: jillcrossman@trentu.ca

N. J. Casson
Department of Geography, University of Winnipeg, Portage Avenue, Winnipeg, MN R3B 2E9, Canada

D. A. Burns
New York Water Science Center, US Geological Survey, 425 Jordan Rd., Troy, New York 12180, USA

J. L. Campbell
Northern Research Station, USDA Forest Service, 271 Mast Rd, Durham, NH 03824, USA

G. E. Likens
Cary Institute of Ecosystem Studies, Millbrook, NY 12545, USA

G. E. Likens
Department of Ecology and Evolutionary Biology, University of Connecticut, Storrs 06269, USA

M. J. Mitchell
State University of New York, College of Environmental Science and Forestry, Syracuse, New York 13210, USA

S. J. Nelson
School of Forest Resources, University of Maine, 5755 Nutting Hall, Orono, ME 04469, USA

This research suggests that catchment response to changes in N deposition is sensitive to climate change; a vulnerability which appears to vary in intensity throughout the seasonally snow-covered temperate region. Furthermore, the sensitivity of stream N-NO_3 export to ROS events and potential shifts (earlier) in the timing of N-NO_3 export relative to other nutrients affect downstream nutrient stoichiometry and the community composition of phytoplankton and other algae.

Keywords Rain-on-snow · Nitrate · Meteorological drivers

Introduction

Climate change projections for the seasonally snow-covered portion of northeastern North America suggest that seasonality of streamflow will likely be impacted by increasing winter temperatures (Barnett et al. 2005; Hayhoe et al. 2007). Warmer winters could have a range of associated effects, many of which have already been observed over the 20th century (Cayan et al. 2001), including significant advances in the timing of spring snowmelt (as indicated by the date of winter-spring center of volume; Hodgkins and Dudley 2006) and increases in the proportion of rain versus snow (Huntington et al. 2004). Meteorological changes during the so-called 'dormant' season could have substantial impacts on soil biogeochemical cycling and surface water quality (Campbell et al. 2010), and stream nitrate (N-NO_3) concentrations appear to be particularly sensitive to winter events. For example, high stream N-NO_3 concentrations following extreme soil frost events have been attributed to declines in the depth of insulating snow cover, which disrupt soil microbial processes, alter soil structure, reduce root uptake, and cause increases in fine root turnover (Mitchell et al. 1996; Fitzhugh et al. 2001; Campbell et al. 2014). Rain-on-snow events also have been associated with substantial stream N-NO_3 export, as both the snowpack and winter rain events are relatively enriched in NO_3, which appear to be transported rapidly to streams in winter runoff, with limited soil interactions (Maclean et al. 1995; Eimers et al. 2007; Sebestyen et al. 2008; Casson et al. 2010). These studies have also shown that N-NO_3 exported in ROS events can deplete the snowpack N pool, resulting in a lower proportion of N-NO_3 being exported in the ensuing spring melt event, which typically accounts for 30–60 % of annual stream flow (e.g. Casson et al. 2010; Likens 2013). In contrast, ROS events are not an important source of either phosphorus (TP) or dissolved organic carbon (DOC) export to stream water—suggesting that nutrient stoichiometry (e.g. N:P ratios) in surface waters may be altered in years with substantial ROS N-export (Casson et al. 2012). Alterations in this stoichiometry can affect phytoplankton species composition (Sickman et al. 2003; Hendzel et al. 2011); even small changes in N-NO_3 ratios can have significant impacts (Sheibley et al. 2014), including increased growth of N-limited species such as cyanobacteria (Nelson 2009). Pulses in N-NO_3 export following ROS events are also associated with substantial declines in stream pH and alkalinity (Eimers et al. 2007), with potential consequences for aquatic life (e.g. Baldigo and Mudoch 1997).

Whilst current global N-NO_3 deposition rates are approximately half of 1990s levels (Vet et al. 2014) owing to declines in emissions occurring since around the beginning of the 21st century, the response of stream N-NO_3 has been variable (Kothawala et al. 2011). Some studies have reported an immediate response in stream water N-NO_3 concentration to declines in deposition (e.g. Kothawala et al. 2011), while at other sites declines in stream water N-NO_3 preceded those in deposition (Goodale et al. 2003), leading to substantial uncertainty over the prevalence of regional drivers. As stream N-NO_3 concentrations in catchments within northeastern North America tend to be highest during the winter-spring period, and the bulk of annual N-NO_3 export occurs during the spring snow melt, changes in winter-spring N dynamics may help to explain some of the spatial and temporal variability in stream N-NO_3 concentrations. However, with the exception of a few sites in south-central

J. B. Shanley
New England Water Science Center, US Geological Survey, 331 Commerce Way, Pembroke, NH 03275, USA

S. A. Watmough
Environmental and Resource Studies Program, Trent University, Peterborough, ON K9J 7B8, Canada

K. L. Webster
Natural Resources Canada, Canadian Forest Service, 1219 Queen St. E, Sault Ste. Marie, ON P6A 2E5, Canada

Ontario, the contribution of ROS events to stream $N\text{-}NO_3$ budgets, and their sensitivity to climate change, has not been evaluated, and importantly there have been few large-scale regional investigations of the drivers of winter-spring $N\text{-}NO_3$ export.

Therefore, this study was designed to answer the following questions:

- Does winter ROS-N export constitute a significant component of annual $N\text{-}NO_3$ export across Ontario and the northeastern United States?
- Does winter ROS-N affect winter in-stream pH and Al concentrations at all catchments?
- What are the *regional* meteorological drivers affecting interannual variability in winter ROS-N export?
- Does the magnitude of winter $N\text{-}NO_3$ export sourced from ROS events influence the magnitude of the ensuing spring $N\text{-}NO_3$ pulse across all catchments?

Methods

Site description

The nine study sites (Fig. 1) are 1st to 3rd order catchments, and span gradients of $N\text{-}NO_3$ deposition, winter temperature, precipitation, length of snow-cover and magnitude of the spring freshet (Table 1). The 20-year period 1990/91–2009/10 (hydrological year: June 1–May 31) was selected for analysis because it is the period of longest coincident monitoring across sites. Catchment areas range from 6.7 to 990 ha. All sites are predominantly forested, though sites TLW37, SR, PC and BBWM contain larger areas of forested wetlands, covering between 5 and 12 % of each catchment. All sites have a temperate climate (Köppen-Geiger Dfb), although site ELA is significantly cooler and drier (by 5.3 °C and 172 mm) than the study-wide annual average. Average winter (December-February) temperatures over the hydrological year 1990/91–2009/10 ranged from −13.3 °C (ELA) to −5.8 °C (CT), and average summer (June- August) temperatures ranged from 16.7 °C (ELA) to 19.3 °C (BBWM). Mean annual precipitation ranged from 745 mm (ELA) to 1658 mm (CT), of which 10 % (ELA) and 16 % (CT) fell as snow between the months of December and February. Of total annual runoff, 37 to 58 % was delivered during the spring (March- May; Online supplementary material 2a); this time period also accounted for 45 to 80 % of the annual $N\text{-}NO_3$ load (Online supplementary material 2b). Average in-stream pH and Al concentrations during winter ranged from 4.4 and 380 µg/l respectively (PC) to 7.7 (SR) and 29.2 µg/l (TLW32).

Identification and quantification of winter ROS events

To identify ROS events, winter meteorological data were analysed from 1990/91 to 2009/10 at all study sites; with the exception of site SR where records began in 1991. Precipitation solute fluxes were calculated using monthly average concentrations collected from monitoring stations located within the study watersheds, multiplied by observed total monthly precipitation; with the exception of site BBWM, where monthly input fluxes were calculated using methods described in Kahl et al. (1999). Although daily stream flow data were available, the frequency of in-stream chemistry sampling ranged from sub-daily to weekly (additional site-specific monitoring details are provided in Online supplementary material 1). Thus the midpoint method (Scheider et al. 1978) was used at all sites to calculate daily stream chemistry data ($N\text{-}NO_3$, Al and pH) from available records, where an unknown concentration was assumed to equal that of the closest sampling date (Casson et al. 2010; O'Connor et al. 2011). Daily stream $N\text{-}NO_3$ concentrations were then multiplied by daily stream flow to obtain stream exports. This same method was used in all streams in order to ensure consistency across stations. As a result, the stream export values of some sites reported here may differ slightly from those published previously.

ROS events were calculated using precipitation, temperature, snowpack depth and stream flow data. Where local meteorological stations did not supply rainfall data separate from that of total precipitation, and in the absence of daily snowfall measurements, proportions of precipitation falling as rain and snow were derived from observed temperature and precipitation records using a simple degree-day snowmelt model, described in more detail in Kokkonen et al. (2006). In summary, below a threshold "snowfall" temperature, all precipitation was assumed to fall as snow. Above this threshold, proportions of precipitation were simulated as rainfall, which increased linearly with air temperature.

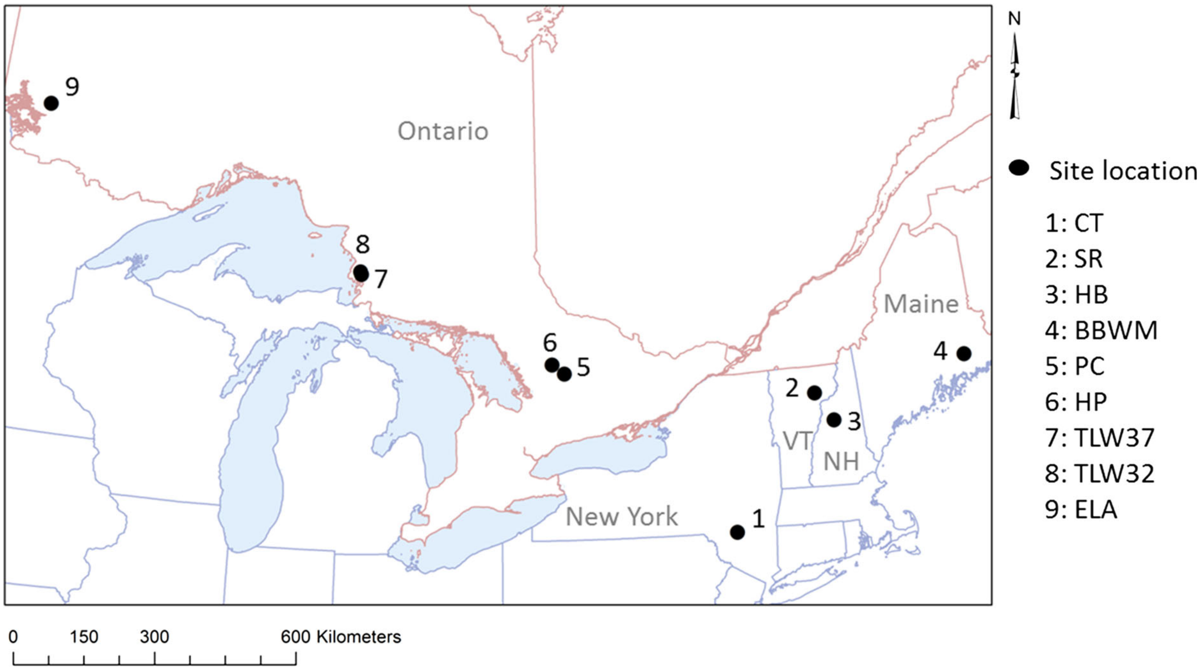

Fig. 1 Site schematic of catchment locations throughout southeastern Ontario and the northeastern United States. Provincial and State boundary files provided by Statistics Canada (2011) and the United States Census Bureau (2014). (*CT* Catskills, *SR* Sleepers River, *HB* Hubbard Brook, *BBWM* Bear Brook Watershed Mainem, *PC* Plastic, *HP* Harp, *TLW37* Turkey Lakes Watershed37, *TLW32* Turkey Lakes Watershed32, *ELA* Experimental Lakes Area)

Snowmelt was simulated as a melt rate (mm/day) occurring above a threshold "snowmelt" temperature. The simulated snowmelt temperature thresholds at the 9 study sites ranged from −0.5 to 4 °C; likely due at least in part to differences between the location of the meteorological station and that of snowpack measurement (e.g. in elevation) (Fontaine et al. 2002). Snowpack accumulation was simulated using the daily mass balance of snow fall minus snowmelt. Results were validated using observed data, including snow pack depth measurements (Online supplementary material 3) and, where available, daily snow fall (cm). Correction coefficients were included in the model, both for rainfall and for snowmelt; to allow for localised effects such as wind, forest interception and orographic enhancement over rain gauges (Fontaine et al. 2002; Kokkonen et al. 2006).

Using this snow accumulation (snowpack depth) and rainfall data, occasions when rainfall occurred on snow covered ground were identified and each hydrograph was visually inspected for a rapid increase in flow following the methods of Casson et al. (2010). When a peak in flow was observed, precipitation from ROS events (ROS-P) was quantified as the daily input of rainfall (mm); and discharge (ROS-Q) and N-NO_3 export (ROS-N) from the event were quantified as the sums of daily fluxes over the duration of the event hydrograph (Eimers et al. 2007). Total seasonal and annual N-NO_3 exports were also calculated to quantify the relative significance of winter ROS-N events. In addition, both the maximum in-stream Al concentrations and minimum stream pH during ROS-Q events, and average winter conditions were calculated. The frequency and volume of ROS-P events were calculated as the annual total number of ROS-P events and annual total volume of rainfall originating from ROS events respectively.

Identification of regional drivers of winter ROS events

To identify relationships between meteorological variables and ROS events at each site, a bivariate correlation matrix was initially applied across ROS events and associated winter meteorological conditions for all years between 1990/91 and 2009/10. The bivariate analysis was also applied across all sites, to determine the spatial variability in relationships. All meteorological variables

Table 1 Mean catchment conditions during winter (Dec–Feb) over a 20 year period (1990/91–2009/10)

	Catchment Area (ha)	Avg winter temp (°C)	Total winter precip (mm)	Rainfall (% of total winter precip)	Daily winter snowpack depth (cm)	Proportion of year with snow cover (%)	$N\text{-}NO_3$ deposition in winter (kg/ha)	Winter $N\text{-}NO_3$ concentration (mg/L)	Winter Al concentration (μg/L)	Winter pH
ELA	56.4	−13	77	4.2	34.6	43.1	1.14	0.02	No data	5.0
(SE ±)		0.52	5.56	1.5	2.3	1.0	0.06	0.01		0.05
TLW32	6.7	−8.4	256	24.6	42.4	35.0	1.19	0.80	29.2	7.2
(SE ±)		0.42	12.0	1.8	3.7	1.2	0.05	0.07	3.5	0.03
TLW37	15.9	−8.4	256	24.6	42.4	35.0	1.19	0.35	63.8	6.9
(SE ±)		0.42	12.0	1.8	3.7	1.2	0.05	0.02	5.9	0.02
HP3a	19.6	−8.3	221	40.0	26.7	35.6	1.24	0.15	97.2	5.9
(SE ±)		0.40	14.7	3.1	3.3	1.1	0.08	0.02	3.4	0.02
PC	23.3	−7.9	221	26.3	39.0	38.9	1.24	0.05	380	4.4
(SE ±)		0.42	13.1	2.2	3.3	1.2	0.08	0.01	24.8	0.02
BBWM	10.9	−5.9	228	56.7	8.6	22.4	0.59	0.04	134	5.7
(SE ±)		0.35	9.6	2.9	1.0	1.1	0.06	0.01	7.6	0.05
SR	40.5	−8.4	290	28.3	54.6	39.9	1.11	0.21	58.3	7.7
(SE ±)		0.40	10.6	2.6	5.2	1.1	0.08	0.02	14.4	0.03
HB	13.2	−6.0	330	45.6	29.7	32.8	1.05	0.08	< detection	5.1
(SE ±)		0.34	13.5	2.7	3.4	1.0	0.06	0.02		0.02
CT	990	−5.8	359	55.8	19.3	32.0	1.00	0.34	66.6	5.9
(SE ±)		0.36	15.9	2.7	3.1	1.0	0.11	0.03	6.2	0.04

were analysed for normality using Q–Q plots and the Shapiro-Wilks test. Whilst many of the variables were normally distributed (average winter temperature, wet-day temperature, total winter precipitation, proportion of winter rainfall, %winter snowcover); those variables which did not meet the assumptions of normality (altitude, latitude, catchment area, %N deposition occurring in winter, snowpack depth, number of winter wet-days with snowcover) were transformed prior to inclusion in the correlation matrix using a Box-Cox power transformation (Box and Cox 1964; Poole et al. 2006). Similarly, ROS event variables (event magnitude, annual discharge, and annual N-export) were Box-Cox transformed. Bivariate correlations were also used to establish any regional similarities in meteorological variability.

A generalised linear model (GLM) with partial factorial analysis was used to identify regional drivers, providing further insight into the spatial (between catchments) and temporal variance in predictor/response relationships. Unlike a standard linear model, a GLM can be applied to non-normally distributed, or even categorised independent variables, and can be used to consider non-linear associations and interactions between predictor variables upon the response variable (Nelder and Wedderburn 1972). For example, in this study the GLM enables exploration of variability in relationships between the meteorological predictor and the ROS dependent variable across various elevations and latitudes. The GLM can also be applied across unequal groups (e.g. where periods of record vary between sites). This was important for the GLM of ROS-N %, as $N\text{-}NO_3$ deposition data for site ELA was available only until 2004–2005.

The normally distributed meteorological variables which had been identified using the bivariate matrix as being significant to site-specific ROS processes were entered as predictor variables into the GLMs, with non-normal ROS event data as dependent variables. Only those predictors that contributed significantly to the GLM ($p < 0.01$) were retained, and re-run in a final GLM. Total model accuracy (R^2) was assessed by comparing model predictions across all sites and years (1990/91–2009/10) with observed data. The site-specific, temporal accuracy was calculated by comparing annual model predictions to observations within each site; and spatial accuracy by comparing variability in site average conditions (20 year), to those of the observed data.

Identifying the impact of winter ROS events on spring exports

The date at which 50 % of the seasonal flow and chemical mass has been exported, referred to as the centre of volume and centre of mass respectively, (Court 1962), was used to assess any redistribution in timing of winter/spring nutrient export (Casson et al. 2012). At each site over the 20-year period, the difference in timing between dates of centre of volume (COV) and centre of mass (COM-N) was quantified. These differences were then compared with ROS-Q and ROS-N, to determine whether ROS-N export influenced the seasonal distribution of $N\text{-}NO_3$ export. To calculate COV and COM-N, daily flow volumes and $N\text{-}NO_3$ exports from January 1st to May 31st of each year were summed, and the date of COV (or COM-N) computed as the date by which half of the volume (or $N\text{-}NO_3$ export) occurred. These dates were selected to avoid the concealment of snowmelt signals by high flows in fall (Hodgkins and Dudley 2006).

Results

Regional Quantification of winter ROS-N events

Over the 20-year period (1990/91–2009/10), spring (Mar–May) was the period of highest flow and $N\text{-}NO_3$ export at all sites (Online supplementary material 2a, 2b), with a regional average contribution to annual flow of 50 %, and to annual $N\text{-}NO_3$ export of 62 %. However, with the exception of ELA, winter (Dec–Feb) also yielded a high proportion of annual flow and $N\text{-}NO_3$ export at all catchments, with regional averages of 18 % and 23 % respectively.

A large proportion of annual precipitation occurred during the winter, with a regional average of 21 % across the nine study sites. Thirty-four percent of winter precipitation fell as rain, of which only 17 % fell on top of an established snowpack thus qualifying as a ROS event (Fig. 2a). Notably fewer ROS events occurred annually at site ELA (0.4) compared with the regional average (3.0 per year) (Fig. 2b). This site had significantly lower mean winter temperature, total precipitation, and a very low proportion of winter rainfall (Table 1). The average daily temperature during ROS events was 0.2 °C, although this ranged from -2.2 °C at ELA to 2.2 °C at PC. At most study

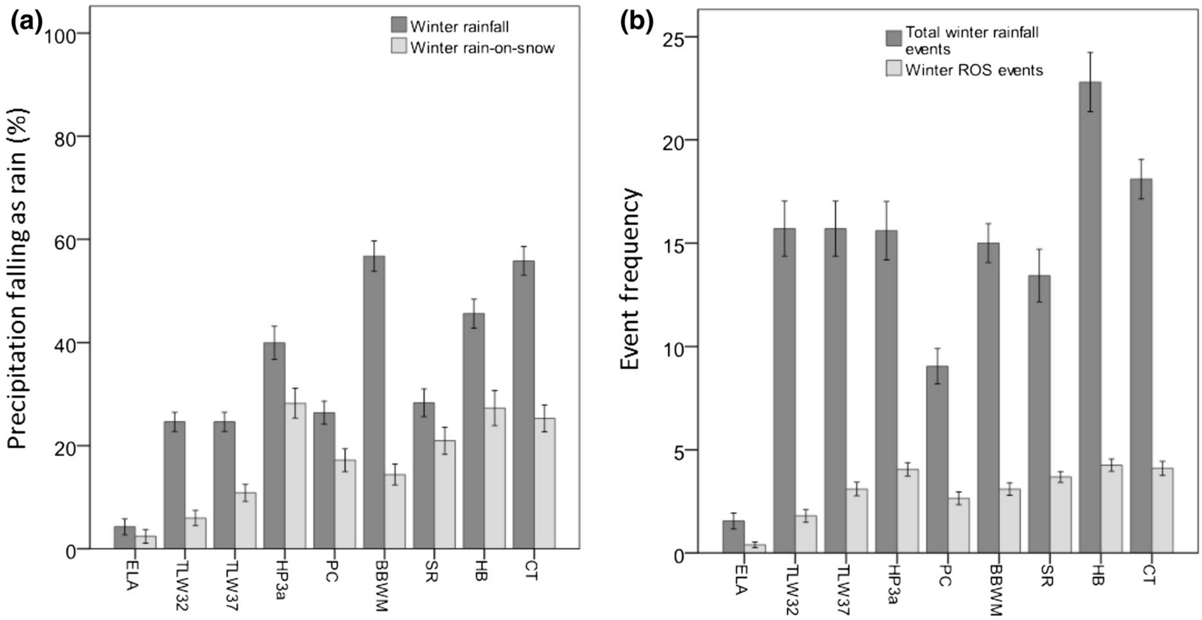

Fig. 2 **a** comparisons between mean (± SE) proportion of winter precipitation falling as rainfall (ROS-P), and mean (± SE) proportion of winter precipitation falling as rain-on-snow events (%); **b** comparison between the mean (± SE) seasonal number of winter rainfall events and mean (± SE) seasonal number of rain-on-snow events (values calculated over 1990/91–2009/10)

sites, ROS events constituted a significant proportion of winter flow (ROS-Q $\%_{winter}$) and of N-NO_3 export (ROS-N $\%_{winter}$) (Fig. 3a, b) with regional averages of 39 % and 42 % respectively. Proportional contributions from ROS events (Q and N-NO_3) from all but two sites fell within ± 1 SD of a regional average.

Impacts of ROS events upon in-stream Al and pH

Stream pH declined during ROS events by an average of 1.5 %, with the exception of site ELA (Fig. 4a) although the difference in stream pH between ROS and average winter conditions was only significant at site CT. Similarly, at sites where in-stream aluminium concentrations were monitored, a high concentration pulse was observed during ROS events relative to average winter conditions (average of +12.2 %) with the exception of ELA (Fig. 4b). Again, the difference was significant only at site CT. These pulses should be considered a conservative estimate, however, as only during periods of high sampling frequency were the direct impacts of ROS-N on stream pH and Al concentrations clearly observed (Fig. 5).

Meteorological drivers of winter ROS events

Regional bivariate trends

Despite the significant difference in average values between sites, cross-site correlations indicated a degree of regional temporal coherence in some meteorological conditions. These included significant correlations ($p < 0.01$) between all sites for winter temperature (Fig. 6a), and for N- deposition (kg/ha). With the exception of ELA and the TLW sites, there was also a significant site association for total winter precipitation (Fig. 6b), and for spring COV (Fig. 6c). Other variables, such as snowpack depth, ROS-P $\%_{annual}$, ROS-N $\%_{winter}$ and COM-N demonstrated some coherence between a more limited number of sites, but were not regionally correlated.

Regional bivariate interactions

Spatial relationships across the 9 study sites demonstrated a positive correlation between ROS frequency and the proportion of winter precipitation falling as rain (%), average winter temperature (^{o}C) and with total winter precipitation (mm), ($p < 0.01$)

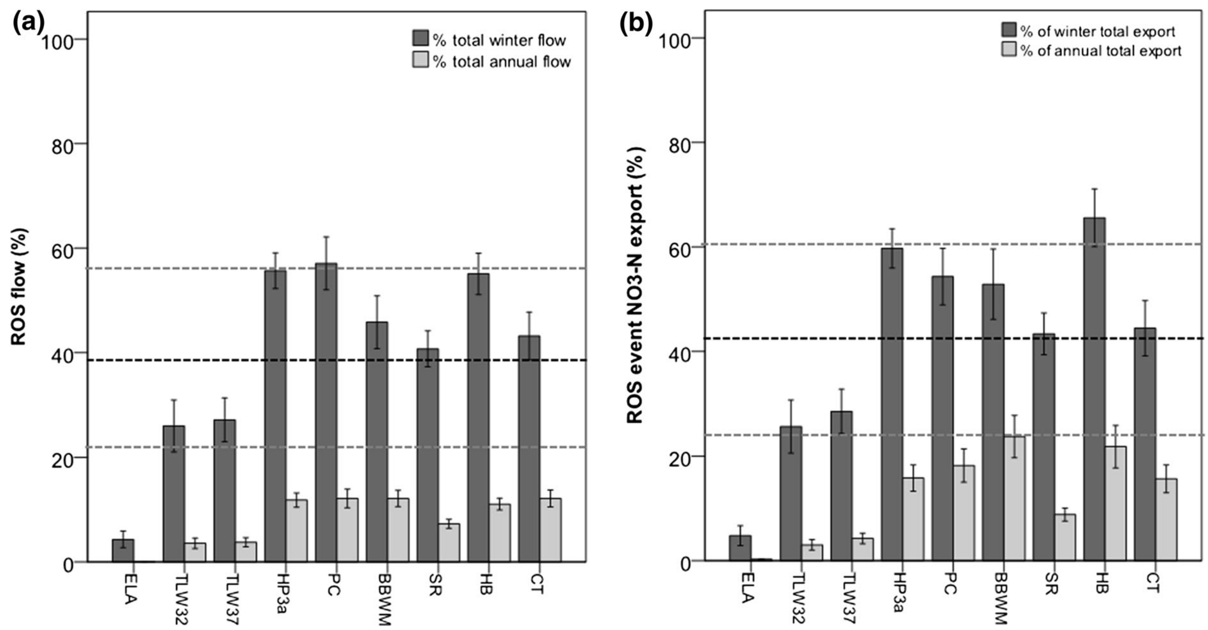

Fig. 3 Comparisons between proportional contributions from ROS events to winter and annual totals of **a** flow and **b** NO_3-N export. Values represent mean (± 1SE) over 1990/1991–2009/2010. (*Black dashed line* study-wide average value of **a** winter ROS flow (%) and **b** winter ROS N-NO_3 export (%), *grey dashed line* ± 1SD study-wide average winter value)

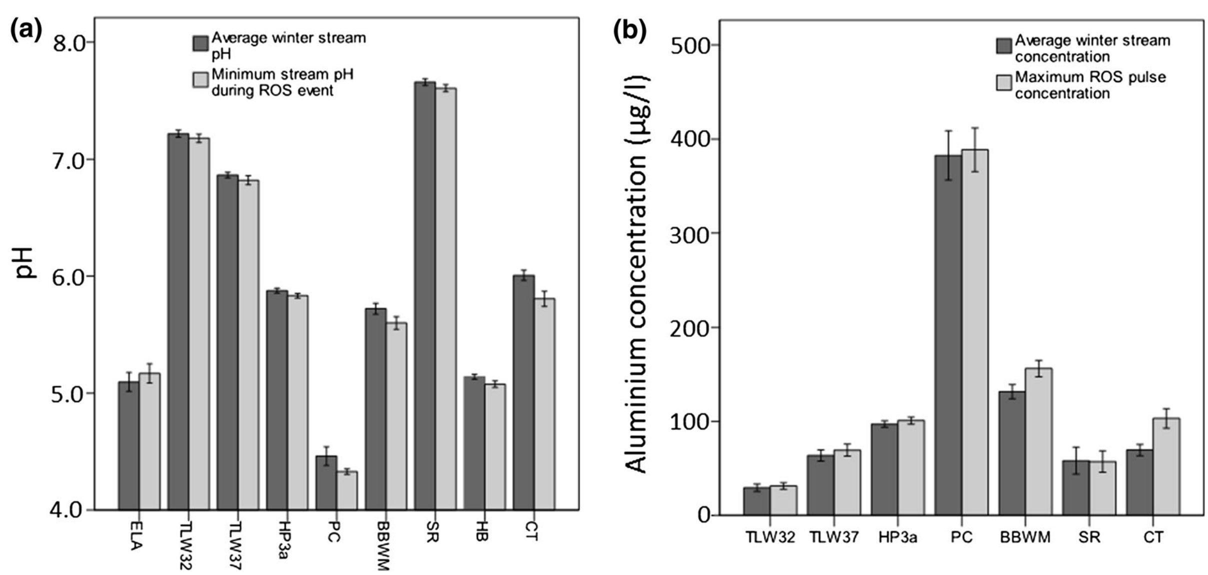

Fig. 4 Comparisons of stream properties between average winter conditions and ROS events for **a** pH and **b** Al concentration (mg/l). Values represent mean (± 1SE) over 1990/91–2009/10

(Figs. 7a,b). However observations at one site, ELA, contained significantly lower average winter temperature, precipitation amounts and a comparatively low 20 year average ROS event frequency and exclusion of the ELA site from the analysis rendered these associations insignificant. There were also significant positive correlations between the proportion of annual precipitation falling as ROS events (ROS-P $\%_{annual}$) and the proportion of annual discharge sourced from ROS events (ROS-Q $\%_{annual}$), and between ROS-

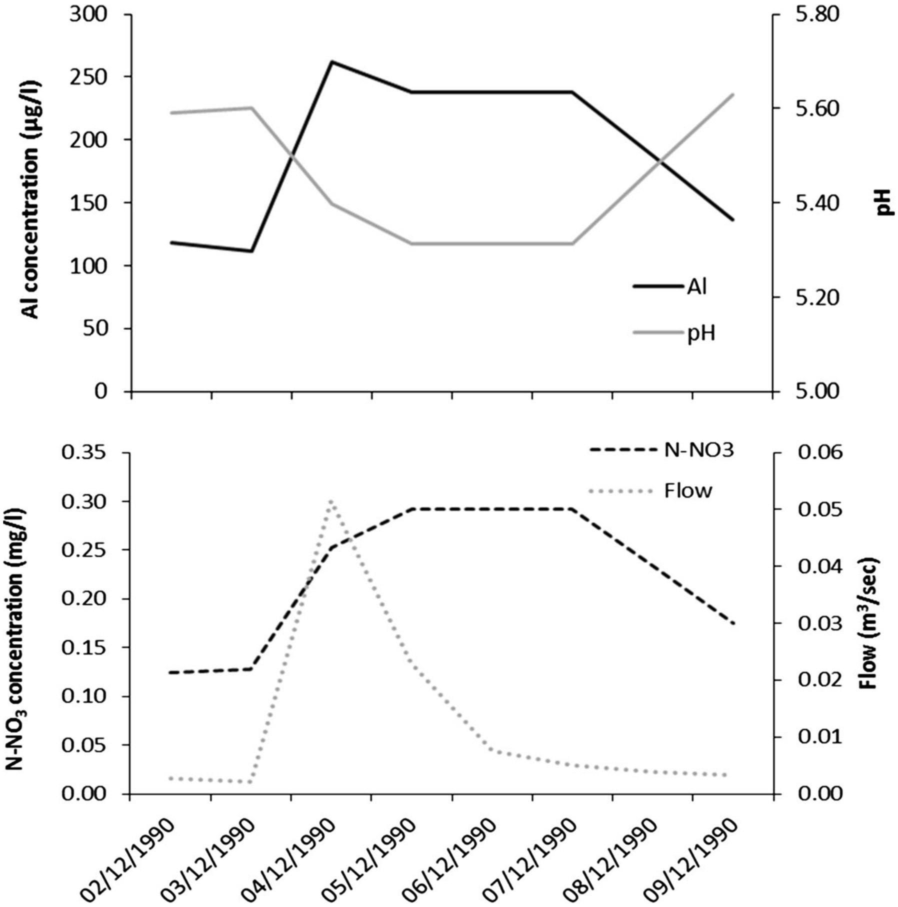

Fig. 5 A week of daily observed water chemistry data demonstrating pulses of elevated Al and associated reduction in pH released from site BBWM during ROS events of high N-NO_3 concentrations (December 2nd–December 9th, 1990)

P $_{\%annual}$ and the proportion of annual N-NO_3 export sourced from the ROS events (ROS-N $\%_{annual}$) ($p < 0.01$). In other words, sites where a greater proportion of annual precipitation and discharge were sourced from ROS events, released a higher proportion of annual N-NO_3 load from these events (Fig. 8a, b). The same relationships were observed when analysing only winter proportions (i.e. ROS-P $\%_{winter}$, ROS-Q $\%_{winter}$ and ROS-N $\%_{winter}$).

Site specific bivariate interactions

Temporal relationships between ROS events (event frequency and rainfall volume) and meteorological drivers differed between sites. A site-specific, bivariate correlation matrix demonstrated significant relationships at some locations, between temporal variance in ROS events (frequency and volume) and in snowpack depth, total winter precipitation, proportions of precipitation falling as rain and %winter snow coverage; whereby higher quantities of precipitation, and a deeper snowpack with persistent coverage increased the probability that a winter rainfall event would occur on snow-covered ground (Table 2). Whilst average winter temperature was only directly associated with ROS events at sites ELA and HP, it was significantly correlated with many of the other meteorological variables. For example, significant correlations between temperature and at least one of either rainfall proportion (+ ve), winter snowmelt (− ve), snow coverage (− ve) and snowpack depth (− ve) were observed at eight of the nine sites (Table 2), indicating that whilst an increase in temperature significantly increased the proportion of winter precipitation falling as rain, it simultaneously acted to reduce snowpack depth and the period of snow coverage. At all sites with the exception of site HP3, significant relationships were also observed between ROS-P $\%_{annual}$ and ROS-Q $\%_{annual}$, and between ROS-P $_{\%annual}$ and ROS-N $\%_{annual}$. ROS-N

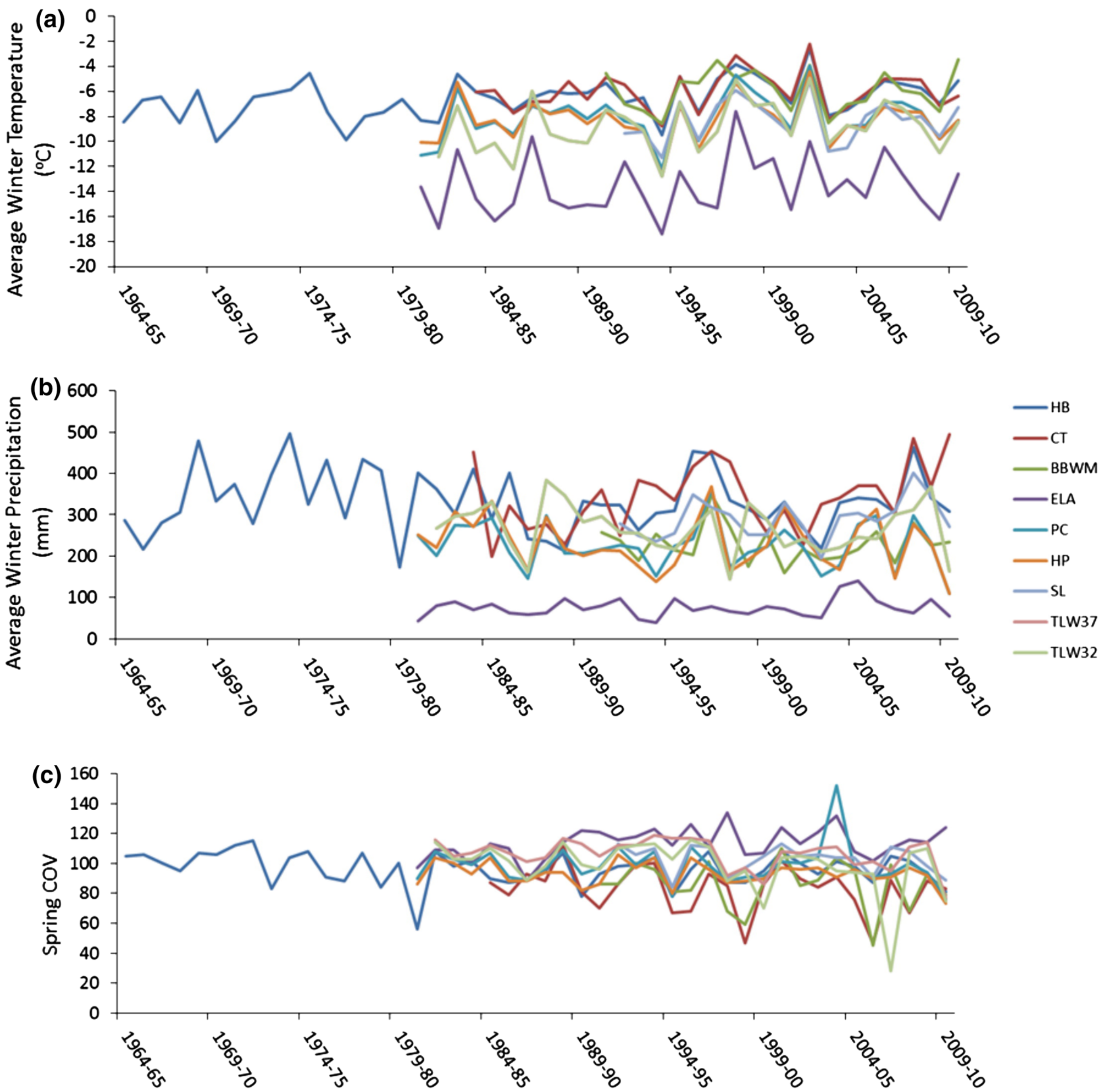

Fig. 6 Regional temporal coherence in **a** winter temperature, **b** total winter precipitation and **c** spring centre of volume

loads (kg) were positively associated with winter N-load deposition (kg/ha) only at site HP ($p < 0.05$), and with winter N-load deposition concentrations (mg/l) only at site HB ($p < 0.05$).

Partial factorial analysis: ROS frequency, magnitude, ROS-Q and ROS-N

The GLM enabled a regional quantification of meteorological ROS drivers, whilst taking into account the site-specific nature of some inter-relationships between drivers, and was applied to each of the primary dependent variables (ROS-P $\%_{winter}$, ROS-frequency, ROS-Q $\%_{winter}$, and ROS-N $\%_{winter}$; Table 3). Combinations of interacting meteorological drivers accounted for up to 87 % of the spatial variance in winter ROS-P $\%_{winter}$ and 89 % of the spatial variance in ROS-frequency. Model accuracy varied amongst sites with respect to the ability to reproduce temporal variance; though significant relationships were determined

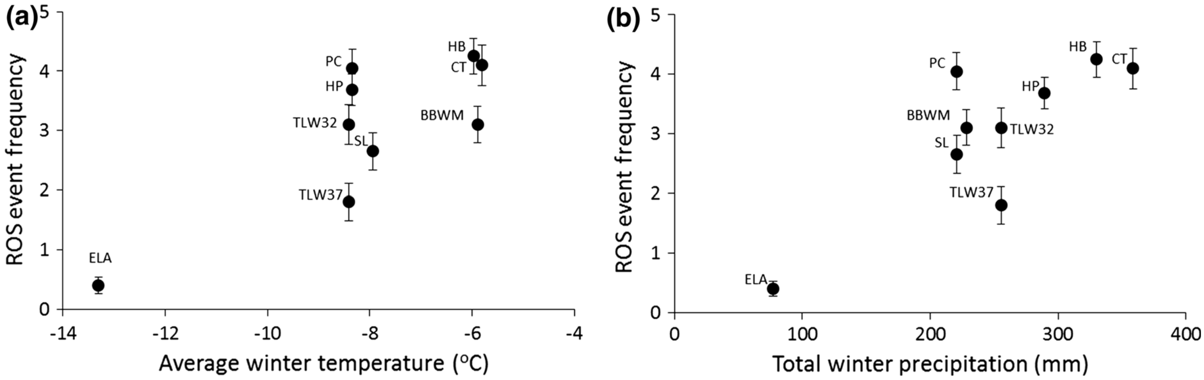

Fig. 7 Mean ± standard error ROS event frequency versus **a** average winter temperature (°C) and **b** total winter precipitation of nine study sites; calculated over 1990/91–2009/10

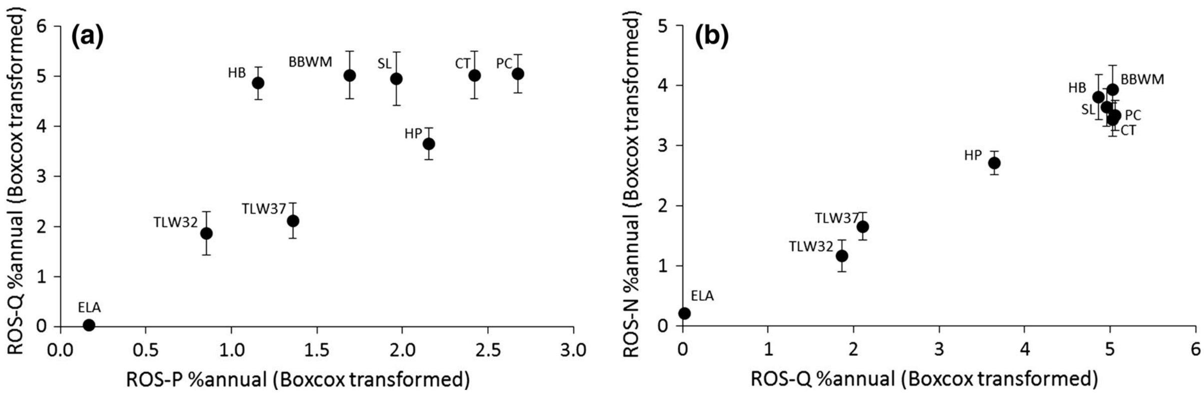

Fig. 8 **a** Mean ± standard error of the proportion of annual discharge sourced from ROS events (ROS-Q %annual) versus the proportion of annual precipitation attributed to ROS events (ROS-P %annual) **b** Mean ± standard error proportion of annual NO3-N export sourced from ROS events (ROS-N %annual) versus ROS-Q %annual. Values calculated over 1990/91–2009/10

between the meteorological drivers and ROS-P $\%_{winter}$ at seven of the nine study sites.

The GLM indicated that ROS event frequency and ROS-P $\%_{winter}$ (i.e. magnitude) were generally lower in sites located farther north (negative correlation with latitude), and that frequency was also lower at sites located at higher elevations (negative correlation with altitude) (Table 3, Online supplementary material 4). Relationships highlighted by the GLM also suggest a positive temporal relationship between ROS-magnitude/frequency and a combined factor of deeper snowpacks with higher winter rainfall proportions. Temperature (winter wet day temperature and average winter temperature) featured in both models, combined with rainfall proportions, though with contrasting associations in the ROS event magnitude GLM to those in the ROS-frequency GLM. Finally, the period of winter snow cover was significantly positively associated with both ROS event frequency and ROS magnitude. Event frequency was additionally impacted by altitude and latitude, and event magnitude by total winter rainfall proportions (Table 3, Online supplementary material 4).

A GLM was able to account for 80 % of the spatial variance in ROS-Q $\%_{winter}$ and 71 % of the spatial variance in winter ROS-N $\%_{winter}$. Whilst temporal accuracy of the models varied amongst sites, both were significant in all areas, and accounted for up to 80 % of temporal variance. The GLM indicated that ROS-N $\%_{winter}$ is greater during winters with higher N deposition and a greater proportional contribution from ROS-Q.

Table 2 A correlation matrix of meteorological and hydrological variables with significant associations with ROS events over the period 1990/91–2009/10

	ROS-frequency					ROS-volume					Average winter temperature				COV		COM-N	
	AWT	*TWP*	*WSC (%)*	*SPD₁*	*SPD₂*	*AWT*	*TWP*	*%WR*	*WSC (%)*	*SPD₁*	*%WR*	*WSM*	*ASC (%)*	*SPD₂*	*ROS-Q*	*ROS-Q (%)*	*ROS-N*	*ROS-N (%)*
ELA	+				+	+		+			+							
TLW32							+			+			-	-				
TLW37										+			-	-				
HP	+						+			+	+	-	-					-
PC		+					+	+			+				-	-		-
BBWM			+	+							+		-	-				
SR									+	+								
HB		+	+				+		+									-
CT											+	-	-	-	-	-		-

Dark grey areas indicate a significant correlation with a P value ≤0.01; light grey of ≤0.05. "+" indicates a positive association, and "−" indicates a negative association. A white cell demonstrates no significant correlation. (*AWT* average winter temperature °C, *TWP* mm total winter precipitation, *WSC*(%) percentage of winter wet days during which snow depth >0 cm, SPD_1 snow pack depth (cm) during days of winter rainfall, SPD_2 snowpack depth (cm) during days of winter precipitation, *%WR* percentage of winter precipitation falling as rain; *%ASC* percentage of the year during which snow depth >0 cm, *WSM* cm winter snow melt; *ROS-Q ROS* discharge in m3/sec, *%ROS-Q* ROS-discharge as a percentage of annual total Q, *ROS-N* = kg of winter ROS N-NO_3 export, *%ROS-N ROS N-NO_3* export as a percentage of annual total N-NO_3 export, *COV* center of volume, *COM-N* center of mass)

Impact of winter ROS-N upon magnitude of spring N-NO_3 export

The COM-N occurred earlier than COV across all sites with the exception of BBWM where timings were concurrent, and a significant positive relationship was established between the difference in COM-N/COV timing and both ROS-Q $\%_{annual}$ and ROS-N $\%_{annual}$. Bivariate correlations also demonstrated a negative correlation across the study sites, between winter ROS-Q $\%_{annual}$ and COV ($p < 0.01$), and between annual ROS-N $\%_{annual}$ and COM-N ($p < 0.01$) (Fig. 9a, b). Temporally, these relationships were significant at sites HB, CT, PC and HP (Table 2). At several sites there was also a significant negative correlation between temporal variance in winter temperature and COV.

The GLM explained 79 % of spatial variation, and up to 42 % of temporal variation in COV, as well as 82 % and up to 58 % of spatial and temporal variation in COM-N, respectively (Table 3). Spatially, earlier COM-N and COV were associated with sites located further south, and a warmer average winter temperature. Temporally, earlier COV and COM-N were associated with years during which a greater proportion of annual discharge and N-NO_3 export were sourced from winter ROS events (significant at five out of nine study sites).

Discussion

Regional significance of winter ROS-N events

Whilst on average only 3.3 % of annual precipitation fell as rain-on-snow during winter over the study period, this generated an average proportion of catchment annual discharge of 8.2 % and 12 % of the annual N-NO_3 export, indicating that ROS events are a significant source of annual stream flow and N-NO_3 export. Rain-on-snow events are an even more important source of winter N-NO_3 export supplying up to 67 % of stream export, and the importance of these events was found to extend throughout southern Ontario and the northeastern United States. Site ELA proved to be an exception, perhaps due to its location in a continental high pressure zone in northern Ontario where air is typically drier and there are lower quantities of winter precipitation (Baldwin et al. 2000). Whilst ROS events have previously been characterised within central Ontario (Eimers et al.

Table 3 Generalised linear models of ROS events ** significant at the 99 % level $normalised using boxcox prior to analysis

Modelled variable	Parameters included	Total variance explained	Proportion of spatial variance explained	Proportion of temporal variance explained
ROS-P % winter	$Rainy-day snowpack depth (SPD_1)	0.58**	0.87**	ELA: 0.72**
	$latitude (LT)			SR: 0.70**
	proportion of winter precip falling as rain			HP: 0.62**
	(%WR)			
	Winter wet day temperature (WWT)			HB: 0.51**
	Percentage winter snow cover (%WSC)			PC: 0.48**
	Winter snowmelt (SM)			TL37: 0.35**
				BBWM: 0.27*
ROS-frequency	Total winter precipitation (TWP)	0.43**	0.89**	HP: 0.30**
	$Rainy-day snowpack depth (SPD_1)			HB: 0.27*
	$altitude (ALT)			CT: 0.25*
	$latitude (LT)			ELA: 0.21
	proportion of winter precip falling as rain (%WR)			PC: 0.19*
	Average winter temperature (AWT)			
	$days of winter snowcover (WSC)			
ROS-Q % winter	$percentage of winter precipitation from ROS-	0.48**	0.80**	SR: 0.74**
	events (ROS-P %winter)			HB: 0.69**
	Winter snowmelt (SM)			PC: 0.60**
	$Catchment area (CA)			ELA: 0.37*
				CT: 0.35**
				TL32: 0.27*
				TL37: 0.22*
				HP: 0.01
ROS-N %winter	Winter N-deposition kg/ha (NDepLoad)	0.56** 0.43**	0.71**	TL32: 0.90**
				TL37: 0.89**
	$Percentage of winter discharge from ROS			ELA: 0.88**
	events (ROS-Q % winter)			PC: 0.52**
	$Catchment area (CA)			CT: 0.49**
				SR: 0.49**
				HP: 0.42**
				BBWM: 0.41**
				HB: 0.27*
COV	$ percentage of annual discharge from ROS		0.79**	CT: 0.42**
	events (ROSQ %annual)			TL32: 0.27*
	Average winter temperature (AWT)			TL37: 0.27*
	$Latitude (LT)			BBWM: 0.23*
				PC: 0.24*

Table 3 continued

Modelled variable	Parameters included	Total variance explained	Proportion of spatial variance explained	Proportion of temporal variance explained
COM-N	$^{\$}$proportion of annual N load from ROS events	0.45**	0.82**	CT: 0.58**
	(ROS-N % annual)			PC: 0.51**
	Average winter temperature (AWT)			HP: 0.37**
	$^{\$}$Latitude (LT)			HB: 0.32**
				TL32: 0.30**

"Spatial variance" refers to model performance between sites; temporal variance refers to model performance within each site; and "total variance" is a measure of the ability of the model to account for all variance within in the dataset

2007; Casson et al. 2010), this is the first time their significant role in N-NO_3 export has been identified across such a large region.

Impacts of ROS events upon in-stream Al and pH

Stream pH was lower and in-stream Al concentrations were higher during ROS events, compared with average winter in-stream observations. To date this difference in stream chemistry has been significant only at site CT. This site had the greatest winter rainfall volumes, and has previously been identified as being vulnerable to winter-spring nitrate acidification and leaching of Al (Murdoch and Stoddard 1992). Furthermore, as daily and sub-daily water chemistry samples were taken only during isolated periods, the analysis is likely to under-estimate changes in Al and pH during ROS events. These findings should therefore be considered conservative estimates, which support suggestions that ROS as a mechanism for N-NO_3 export could influence the rate of chemical recovery from acidification (Eimers et al. 2007); whereby areas with higher ROS contributions are likely to recover more slowly.

Meteorological drivers of ROS events

Site specific interactions

Site specific bivariate analyses indicated that higher quantities of precipitation, greater snowpack depth and more persistent snow coverage all increased the probability that a winter rainfall event would occur on frozen or snow-covered ground. However, higher temperatures both increased winter rainfall proportions and simultaneously reduced snowpack depth and periods of snow coverage. Use of a generalised linear model, with partial factorial analysis, enabled quantification of these interactive effects. Models of ROS event frequency and magnitude both included winter rainfall proportions and snow cover, indicating that consistent with the findings of Surfleet and Tullos (2013), the impact of rainfall proportions upon ROS events was dependent upon the snowpack conditions. Winter temperature interactions differed between models of ROS-frequency and ROS-magnitude, where increases in temperature and rainfall proportions were associated with a higher ROS event magnitude but reduced frequency of occurrence. This is likely due to the conflicting effects of a higher volume of rainfall occurring in warmer, wetter conditions; whilst a reduction in snow cover results in a greater number of events falling on bare (i.e., not snow covered) ground (McCabe et al. 2007).

Whilst bivariate associations demonstrated positive relationships between ROS-P $\%_{annual}$ and ROS-Q $\%_{annual}$ and in turn with ROS-N $\%_{annual}$, there was little direct correspondence with atmospheric N-NO_3. These results are consistent with findings from Piatek et al. (2005) and Campbell et al. (2002), who demonstrated that atmospheric N deposition alone cannot explain variation in stream N-NO_3 during winter/spring. Although this might be initially interpreted as being due to N deposition levels below critical load thresholds (< 12 kg/ha/year; Aherne and Posch 2013), the results from the GLM indicate that instead, it is important to simultaneously consider variability in ROS event magnitude (e.g. the proportion of winter discharge sourced from ROS) with N deposition. The interactive nature of the relationship between N deposition and ROS-Q suggests that future efforts to reduce winter

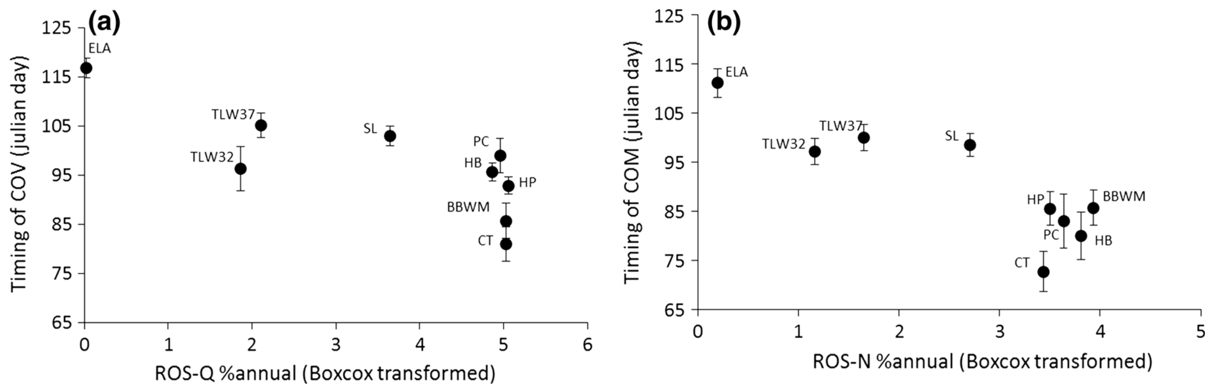

Fig. 9 **a** Mean ± standard error of the timing of spring COV versus ROS-Q % $_{annual}$; **b** mean ± standard error of the timing of spring COM-N versus ROS-N % $_{annual}$. Values calculated over 1990/91–2009/10

N-NO_3 exports will require a concurrent decline in both atmospheric N deposition and the magnitude of winter ROS events. Similar to Baron et al. (2009), these results indicate that interpretation of N-deposition effects is complicated by the co-occurrence of climate change, and should climatic change lead to an increase in ROS event frequency or magnitude (and hence in ROS-Q), reductions in NO_x emissions alone will be unlikely to prevent future increases in winter N-NO_3 exports. ROS-associated reductions in stream pH and increases in Al concentrations could therefore potentially impede stream recovery from acidification, despite reduced atmospheric emissions (Dillon et al. 1988; Eimers et al. 2007).

Regional interactions

Whilst several of the meteorological variables demonstrated a degree of regional coherence (e.g. winter temperature, N deposition, total winter precipitation), temporal variability in ROS-P, ROS-Q and ROS-N was not consistent across study sites. This difference can be attributed to the interactive role of both regionally coherent (e.g., temperature) and more catchment-specific (e.g., snowpack depth) drivers in the ROS processes identified by the GLM. At site ELA, with a notably cooler and drier climate, significantly fewer ROS events were observed (Fig. 7a). However as a result of the site-specific and sometimes contrasting driver interactions, between temperature, rainfall proportions and winter snow coverage, there was also high variability in ROS frequency (Fig. 7a) and magnitude between study sites with statistically similar meteorological conditions (e.g. TLW37, TLW32, SL and PC).

Importantly, these results indicate that sites located in northern temperate regions may exhibit a wide range of vulnerabilities (ROS-responses) to potential changes in meteorological variables; these vulnerabilities are dependent on the site-specific interactive responses of the snowmelt-snow accumulation balance. For example, under an increase in temperature, sites most likely to undergo an increase in ROS-Q and ROS-N are those with a combination of high winter precipitation and deeper winter snowpacks (sites TLW37, TLW32 and SL). Here, ROS magnitude can increase (due to an increase in proportion of winter rainfall), without a reduction in event frequency (because the deep snowpack sustains complete coverage). Sites more resilient to winter climate change are those with exceptionally dry climates (ELA), or shallower snowpacks (HP and BBWM) (Fig. 10). This range in catchment vulnerability to meteorological variables goes some way toward explaining the high variance in water quality responses to changes in N deposition.

Impact of winter ROS-N on spring N-NO_3

Our results show that the timing of both COV and COM-N are associated with temperature, generally occurring later at cooler sites situated farther north. Importantly, COV and COM-N occurred earlier in the year at sites with higher ROS-Q % $_{annual}$ and ROS-N % $_{annual}$, respectively. This, combined with the increasing difference in timing between COM-N and COV under higher ROS event magnitude indicates a general redistribution of available N to earlier in the season, where an earlier COM-N results not solely

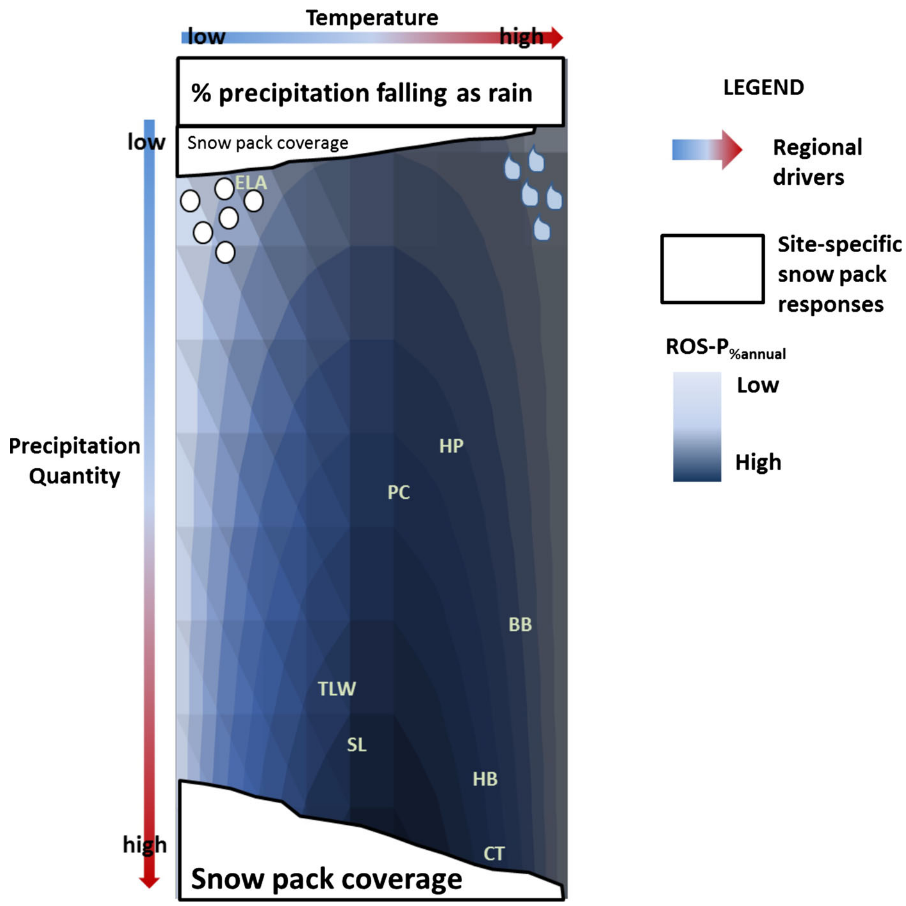

Fig. 10 Conceptual diagram of interactive effects of regional and site-specific meteorological drivers upon ROS events across Ontario and northeastern USA

from a change in hydrological export, but also from an earlier release of N-NO_3 during winter ROS events (Casson et al. 2012). The significant negative temporal correlation between ROS-N load (both $\%_{annual}$ and absolute kg) and timing of COM-N supports these findings, indicating that at several sites (HB, CT, PC and HP), temporal variance in the magnitude of winter ROS events significantly influences the timing of spring N-NO_3 export.

An increase in ROS events might therefore be expected to lead to higher N-NO_3 export during the winter and proportionately smaller N-NO_3 export in the spring. Studies in northeastern North America have shown that as other nutrients, such as total phosphorus and dissolved organic carbon, are not sensitive to ROS events (Casson et al. 2012) alterations to stream nutrient stoichiometry might also be anticipated. The timing of N-NO_3 release is important in the aquatic environment, with reductions in spring melt and associated N-NO_3 export having the potential to affect community composition of phytoplankton and other algae (Sickman et al. 2003; Nelson 2009). Changes in N:P ratios are widely accepted to result in alterations to phytoplankton communities (e.g. Hendzel et al. 2011; Shiebley et al. 2014), and can even lead to growth of N_2 fixers such as cyanobacterium (Levine and Schindler 2011) if periods of N-limitation result (N: P < 1.5; Bergstrom 2010). Those sites most vulnerable to change in meteorological variables (in terms of ROS-N responses) should therefore be considered at greatest risk of alterations in stream nutrient stoichiometry.

Conclusion

ROS events contributed up to 24 % of annual stream N-NO_3 export in catchments within southern Ontario and the northeastern US, and were associated with higher in-stream Al concentrations and lower pH. In contrast, site ELA in northern Ontario, with a significantly cooler and drier climate, demonstrated far fewer ROS events, which constituted a much lower proportion of annual N-NO_3 export. In addition, there was a greater difference between the timing of winter/spring COV and winter/spring COM-N in years with ROS events of greater magnitude, indicating that ROS events result in a redistribution of available N-NO_3 to earlier in the spring.

ROS events were associated with winter temperature, precipitation, snowpack depth and persistence of snow coverage. Spatial variability in ROS frequency and magnitude was high, despite some regional similarities in meteorological variables (e.g., similar temporal variance in winter temperature across sites), and can be explained by the substantial influence of highly localised drivers (e.g., snowpack depth). Importantly, these results demonstrate that higher temperatures are likely to result in greater ROS events only where snowpack coverage is not reduced.

The significant localized influence of snowpack characteristics upon ROS interactions with meteorological variables led to the identification of a range of site "vulnerabilities" to changes in winter temperature. The most vulnerable areas (i.e., most likely to experience increases in ROS-N, redistribution of spring N-NO_3, and delayed recovery from acidification) were identified as those with a combination of highest total winter precipitation and deepest winter snowpacks, where temperature increases would increase ROS magnitude without removing snowpack cover. Given the regional significance of these findings, there is potential for increases in ROS-N at vulnerable sites across Ontario and the northeastern US, with associated implications for water quality (stream pH), nutrient stoichiometry, and phytoplankton community structure. Further research is required to quantify potential changes in general water quality and nutrient stoichiometry under plausible future change, and importantly to identify the spatial extent of these most vulnerable locations.

Acknowledgements The authors thank the many agencies that contributed to the long-term data records for these sites. The cross-site comparison was funded by an NSERC Strategic Grant. Monitoring of Harp and Dickie Lake was supported by the Ontario Ministry of Environment and Climate Change, and the Dorset Environmental Science Centre. The long-term data from IISD-ELA represent the hard work of many past and present staff, and are gratefully acknowledged. BBWM data have been collected since 1986 with support from the US EPA, US NSF, USGS, USFS, the Maine Agricultural and Forest Experiment Station, and the University of Maine. Funding for precipitation and streamwater chemistry at Hubbard Brook was provided by the National Science Foundation, including the LTER and LTERB programs, and the A.W. Mellon Foundation; hydrometeorological data were obtained through support from the USDA Forest Service. Data collection at Biscuit Brook is funded by the Long-Term Monitoring Program of the U.S. Environmental Protection Agency. Funding for this research at the TLW sites was provided by Canadian Forest Service base funds.

References

Aherne J, Posch M (2013) Impacts of nitrogen and sulphur deposition on forest ecosystem services in Canada. Curr Opin Environ Sustain 5(1):108–115

Baldigo BP, Mudoch PS (1997) Effect of stream acidification and inorganic aluminium on mortality of brook trout (Salvelinus frontinalis) in the Catskills Mountains, New York. Can J Fish Aquat Sci 54(3):603–615

Baldwin DJB, Desloges JR, Band LE (2000) 2 Physical Geography of Ontario. In: Perera AH, Euler DA, Thompson ID (eds) Ecology of a managed terrestrial landscape: patterns and processes of forest landscapes in Ontario. University of British Columbia Press, Vancouver B.C, pp 141–162

Barnett TP, Adam JC, Lettenmaier DP (2005) Potential impacts of a warming climate on water availability in snow-dominated regions. Nature 438:303–309

Baron JS, Schmidt TM, Hartman MD (2009) Climate-induced changes in high elevation stream nitrate dynamics. Glob Change Biol 15:1777–1789

Beall FD, Semkin RG, Jeffries DS (2001) Trends in the output of first-order basins at Turkey Lakes Watershed, 1982–1996. Ecosystems 4(6):514–526

Beaty KG (1981) Hydrometeorological data for the Experimental Lakes Area, northwestern Ontario, 1969 through 1978. Can Data Rep Fish Aquat 285:367

Bergstrom AK (2010) The use of TN:TP and DIN:TP as indicators for phytoplankton nutrient limitation in oligotrophic lakes affected by N deposition. Aquat Sci 71:277–281

Box GEP, Cox DR (1964) An analysis of transformation. J Roy Stat Soc 26(2):211–252

Burton WC, Walsh GJ, Armstrong TR (2000) Bedrock geologic map of the hubbard brook experimental forest, Grafton County, New Hampshire: US geological survey Open-File Report 00-45. US Geological Survey, Reston, Virginia

Buso DC, Likens GE, Eaton JS (2000) Chemistry of precipitation, streamwater, and lakewater from the Hubbard Brook Ecosystem Study: a record of sampling protocols and analytical procedures. Gen. Tech. Rep. NE-275. Newtown Square, PA: U.S. Department of Agriculture, Forest Service, Northeastern Research Station p 52

Campbell DH, Kendall C, Chang CCY, Silva SR (2002) Pathways for nitrate release from an alpine watershed: determination using δ^{15}N and δ ^{18}O. Water Resour Res 38(5):1052–1061

Campbell JL, Ollinger SV, Flerchinger GN, Wicklein H, Hayhoe K, Bailey AS (2010) Past and projected future changes in snowpack and soil frost at the Hubbard Brook

Experimental Forest, New Hampshire. USA Hydrol Process 24(17):2465–2480
Campbell JL, Socci AM, Templer PH (2014) Increased nitrogen leaching following soil freezing is due to decreased root uptake in a northern hardwood forest. Glob Change Biol 20(8):2663–2673
Casson NJ, Eimers MC, Buttle JM (2010) The contribution of rain-on-snow events to nitrate export in the forested landscape of south-central Ontario, Canada. Hydrol Process 24:1985–1993
Casson NJ, Eimers MC, Watmough SA (2012) Impact of winter warming on the timing of nutrient export from forested catchments. Hydrol Process 26:2546–2554
Cayan DR, Kammerdiener SA, Dettinger MD, Caprio JM, Peterson DH (2001) Changes in the onset of spring in the Western United States. Bull Am Meteorol Soc 82:399–415
Court A (1962) Measures of streamflow timing. J Geophys Res 67(11):4335–4339
Dillon PJ, Lusis M, Reid R, Yap D (1988) Ten-year trends in sulphate, nitrate and hydrogen in central Ontario. Atmos Environ 22(5):901–905
Eimers MC, Buttle JM, Watmough SA (2007) The contribution of rain-on-snow events to annual NO_3-N export from a forested catchment in south-central Ontario, Canada. Appl Geochem 22:1105–1110
Fernandez IJ, Rustad LE, Norton SA, Kahl JS, Cosby BJ (2003) Experimental acidification causes soil base-cation depletion at the Bear Brook watershed in Maine. Soil Sci Soc Am J 67(6):1909–1919
Fitzhugh RD, Driscoll CT, Groffman PM, Tierney GL, Fahey TJ, Hardy JP (2001) Effects of soil freezing disturbance on soil solution nitrogen, phosphorus, and carbon chemistry in a northern hardwood ecosystem. Biogeochemistry 56:215–238
Fontaine TA, Cruickshank TS, Arnold JG, Hotchkiss RH (2002) Development of a snowfall-snowmelt routine for mountainous terrain for the soil water assessment tool (SWAT). J Hydrol 262:209–223
Foster N, Spoelstra J, Hazlett P, Schiff S, Beall F, Creed I, David C (2005) Heterogeneity in soil nitrogen within first-order forested catchments in the Turkey Lakes Watershed. Can J For Res 35(4):797–805
Goodale CL, Aber JD, Vitousek PM (2003) An unexpected nitrate decline in New Hampshire streams. Ecosystems 6:75–86
Hayhoe K, Wake CP, Huntington TG, Luo L, Schwartz MD, Sheffield J, Wood E, Anderson B, Bradbury J, DeGaetano A, Troy TJ, Wolfe D (2007) Past and future changes in climate and hydrological indicators in the US Northeast. Clim Dyn 28:381–407
Hendzel LL, Hecky RE, Findlay DL (2011) Recent changes of N2-Fixation in Lake 227 in response to reduction of the N: P loading ratio. Can J Fish Aquat Sci 51(10):2247–2253
Hodgkins GA, Dudley RW (2006) Changes in the timing of winter-spring streamflows in eastern North America, 1913–2002. Hydrol Land Surf Stud. doi:10.1029/2005GL025593
Huntington TG, Hodgkins GA, Keim BD, Dudley RW (2004) Changes in the proportion of precipitation occurring as snow in New England (1949–2000). J Clim 17:2626–2636
Kahl J, Norton S, Fernandez I, Rustad L, Handley M (1999) Nitrogen and sulfur input-output budgets in the experimental and reference watersheds, Bear Brook Watershed in Maine (BBWM). Environ Monit Assess 55(1):113–131
Kokkonen K, Koivusalo H, Jakeman A, Norton J (2006) Construction of a degree-day snow model in the light of the "ten iterative steps in model development". In: Voinoc A, Jakeman AJ, Rizzoli AE (eds) Proceedings of the iEMSs third biennial meeting: "summit on environmental modelling and software". International Environmental Modelling and Software Society, Burlington
Kothawala DN, Watmough SA, Futter MN, Zhang L, Dillon PJ (2011) Stream nitrate responds rapidly to decreasing nitrate deposition. Ecosystems 14:274–286
Laird KR, Cumming BF (2008) Reconstruction of Holocene lake levels from diatoms, chrysophytes and organic matter in a drainage lake from the Experimental Lakes Area (northwestern Ontario, Canada). Quatern Res 69:292–305
Levine SN, Schindler DW (2011) Influence of nitrogen to phosphorus supply ratios and physicochemical conditions on cyanobacteria and phytoplankton species composition in the Experimental Lakes Area, Canada. Can J Fish Aquat Sci 56(3):451–466
Likens GE (2013) Biogeochemistry of a Forest Ecosystem (3rd Ed.). Springer, NY, p 208
Maclean RA, English MC, Schiff SL (1995) Hydrological and hydrochemical response of a small Canadian Shield catchment to late winter rain-on-snow events. Hydrol Process 9:845–863
Mayer B, Shanley JB, Bailey SW, Mitchell MJ (2010) Identifying sources of stream water sulfate after a summer drought in the Sleepers River watershed (Vermont, USA) using hydrological, chemical and isotopic techniques. Appl Geochem 25:747–754
McCabe GJ, Clark MP, Hay LE (2007) Rain-on-snow events in the Western United States. Bull Am Meteorol Soc 88:319–328
Mitchell MJ, Driscoll CT, Kahl JS, Murdoch PS, Pardo LH (1996) Climatic control of nitrate loss from forested watersheds in the northeast United States. Environ Sci Technol 30:2609–2612
Murdoch PS, Stoddard JL (1992) The role of nitrate in the acidification of streams in the Catskill Mountains of New York. Water Resour Res 28(10):2707–2720
Nelder JA, Wedderburn RWM (1972) Generalized linear models. J Roy Stat Soc 135(3):370–384
Nelson CE (2009) Phenology of high-elevation pelagic bacteria: the roles of meteorological variability, catchment inputs and thermal stratification in structuring communities. ISME J 3:13–30
Norton S, Kahl J, Fernandez I, Haines T, Rustad L, Nodvin S, Scofield J, Strickland T, Erickson H, Wigington P Jr, Lee J (1999) The Bear Brook Watershed, Maine (BBWM). USA. Environ Monit Assess 55(1):7–51
O'Connor EM, McConnell C, Lembcke D, Winter JG (2011) Estimation of total phosphorus loads for a large, flashy river of a highly developed watershed—seasonal and hysteresis effects. J Gt Lakes Res 37:26–35
Piatek KB, Mitchell MJ, Silva SR, Kendall C (2005) Sources of nitrate in snowmelt discharge: evidence from water

chemistry and stable isotopes of nitrate. Water Air Soil Pollut 165:13–35
Poole GG, Stanford JA, Running SW, Frissel CA (2006) Mutiscale geomorphic drivers of groundwater flow paths: subsurface hydrologic dynamics and hyporheic habitat diversity. J N Am Benthol Soci 25(2):288–303
Scheider WA, Moss JJ, Dillon PJ (1978) Measurement and uses of hydraulic and nutrient budgets. Lake Restoration, Proceedings of a national conference; Minneapolis, Minnesota, USA, 22–24 August
Sebestyen SD, Boyer EW, Shanley JB, Kendall C, Doctor DH, Aiken GR, Ohte N (2008) Sources, transformations, and hydrological processes that control stream nitrate and dissolved organic matter concentrations during snowmelt in an upland forest. Water Resour Res 44:W12410. doi:10.1029/2008WR006983
Shanley JB, Sebestyen SD, McDonnell JJ, McGlynn BL, Dunne T (2015) Water's Way at Sleepers River watershed—revisiting flow generation in a post-glacial landscape. Vermont USA. Hydrol Process 29(16):3447–3459
Sheibley RW, Enache M, Swarzenski PW, Moran PW, Foreman JR (2014) Nitrogen deposition effects on diatom communities in lakes from three national parks in Washington State. Water Air Soil Pollut 225:1857–1879
Sickman JO, Melack JM, Clow DW (2003) Evidence for nutrient enrichment of high-elevation lakes in the Sierra Nevada California. Limnol Oceanogr 48:1885–1892
Statistics Canada (2011) Census boundary files. Cartographic provincial boundaries. Available for download at: http://www12.statcan.gc.ca/census-recensement/2011/geo/bound-limit/bound-limit-2011-eng.cfm Accessed 30th August 2015
Surfleet CG, Tullos D (2013) Variability in the effect of climate change on rain-on-snow peak flow events in a temperate climate. J Hydrol 479(4):24–34
United States Census Bureau (2014) Cartographic boundary shapefiles. Available for download at: https://www.census.gov/geo/maps-data/data/cbf/cbf_state.html Accessed 30th August 2015
Vet R, Artz RS, Carou S, Shaw M, Ro C, Aas W, Baker A, Bowersox VC, Dentener F, Galy-Lacaux C, Hou A, Pienaar JJ, Gillett R, Forti MC, Gromov S, Hara H, Khodzher T, Mahowald NM, Nickovic S, Rao PSP, Reid NW (2014) A global assessment of precipitation chemistry and deposition of sulfur, nitrogen, seas salt, base cations, organic acids, acidity and pH, and phosphorus. Atmos Environ 93:3–100
Watmough SA, Dillon PJ (2003a) Base cation and nitrogen budgets for a mixed hardwood catchment in South-central Ontario. Ecosystems 6:675–693
Watmough SA, Dillon PJ (2003b) Base cation and nitrogen budgets for seven forested catchments in central Ontario, 1983-1999. For Ecol Manage 177:155–177